*Refereed Proceedings*

*The 12th International Conference on Fluidization - New Horizons in Fluidization Engineering*

Engineering Conferences International *Year* 2007

# Development of Electrical Capacitance Volume Tomography (ECVT) and Electrostatic Tomography (EST) for 3D Density Imaging of Fluidized Bed System

B. Du[*] Q. Marashdeh[†] W. Warsito[‡]
A.-H. A. Park[**] L S Fan[††]

[*]The Ohio State University
[†]The Ohio State University, marashdeh@gmail.com
[‡]The Ohio State University
[**]The Ohio State University
[††]The Ohio State University, fan@chbmeng.ohio-state.edu

# DEVELOPMENT OF ELECTRICAL CAPACITANCE VOLUME TOMOGRAPHY (ECVT) AND ELECTROSTATIC TOMOGRAPHY (EST) FOR 3D DENSITY IMAGING OF FLUIDIZED BED SYSTEM

Du, B., Marashdeh, Q., Warsito, W., Park, A.-H. A., and Fan, L.-S.
Department of Chemical and Biomolecular Engineering
The Ohio State University, Columbus, OH 43210

## ABSTRACT

In this paper, Electrical Capacitance Volume Tomography (ECVT) is used to study a gas-solid fluidized bed system of .1 m ID. The interior flow structures (including the dynamic bed expansion, bubble/void breakage and particle movement) and the charge distribution in a gas-solid fluidized bed are illustrated based on the 3D images obtained from the ECVT.

## INTRODUCTION

The electrical capacitance volume tomography (ECVT) and the electrostatic tomography (EST) are developed for imaging the 3-D , real time flow field in particulates and multiphase systems (Warsito *et al*., 2006) (Fan *et al*., 2006). The geometrical variation in sensor design that enables the direct 3-D imaging and the Hopfield neural network for image inverse scheme that enables accurate reconstruction of the flow field highlight the uniqueness of the ECVT. The ECVT (Warsito *et al*., 2006) has been extended to imaging volumes of particulate systems which are prevalent in industrial processes. Volume imaging of particulate system is conducted by placing 3D capacitance sensors around the vessel of interest, and applying the 3D neural-network image reconstruction technique for image reconstruction. This ECVT technique has enabled the exploration of multi-phase and particulate system in three dimensions.

The fluidized bed system under study is a 0.1 m ID gas-solid fluidized bed. The ECVT generates a real-time volume image defined in image voxels (volume pixels) of 20×20×20 resolutions from the capacitance data obtained using a 12-electrode sensor which surrounds the 3D section of 9 cm in length of a cylindrical column. Both of the Geldart Group A particles (FCC catalyst with a mean diameter of 60 $\mu$m and a density of 1400 kg/m$^3$) and Group B particles (glass beads with a mean diameter of 200 $\mu$m and a density of 2500 kg/m$^3$) are employed in the experiments. The interior flow structures (including the dynamic bed expansion, bubble/void breakage and particle movement) and the charge distribution in a gas-solid fluidized bed are illustrated based on the 3D images obtained from the ECVT.

The 12th International Conference on Fluidization - New Horizons in Fluidization Engineering, Art. 57 [2007]

## THEORETICAL APPROACH

### ECVT System

The electric field distribution inside the vessel depends on the permittivity distribution according to Poisson equation 1.

$$\nabla \varepsilon(x,y,z) \nabla \varphi(x,y,z) = -\rho(x,y,z) \quad (1)$$

Here $\varepsilon(x,y,z)$ is the permittivity distribution, $\varphi(x,y,z)$ is the electric field distribution, and $\rho(x,y,z)$ is the charge distribution. And the capacitance between two pairs of electrodes is obtained through solving equation 2.

$$C_i = \frac{1}{\Delta V_i} \oiint_A \varepsilon(x,y,z) \varphi(x,y,z) dA \quad (2)$$

where $C_j$ is the capacitance value between two plates $\Delta V_j$ is the voltage difference between the pair of plates, and A is the surface area surrounding one plate.

ECVT imaging is based on reconstruction of a 3D permittivity distribution directly from the measured capacitance. This task is achieved by acquiring the capacitance signal through a 3D sensor capable of providing a field distribution of 3D variation. The 3D capacitance sensor provides capacitance data with diversity based on the 3D distribution of materials in the imaging domain. The capacitance signal in ECVT technology is acquired through a 3D ECVT sensor. The sensor used in this study is depicted in figure 1.b. The sensor in the figure is composed of 12 electrodes arranged in three shifted planes. The capacitance measurement is acquired between each electrode and the other electrodes in all planes. Thus 66 independent capacitance measurements are obtained; further details about the same sensor are presented in (Warsito *et al*., 2006). The quality of the final image solution depends highly on the image reconstruction technique used to obtain it. In this regard, the neural network multi objective criterion image reconstruction technique for volume tomography (NN-MOIRVT) or 3D NN-MOIRT proved superiority in terms of quality of reconstructed images as well as fast reconstruction speed (Warsito *et al*., 2006). It is important to note that the ECT system refers to the 2D capacitance tomography system whereas the ECVT refers to volume imaging (3D) based on 3D capacitance sensor and 3D image reconstruction technique.

### ECVT Reconstruction Technique

The 3D NN-MOIRT described in (Warsito *et al*., 2006) is based on optimization of four different objective functions related to both the measured capacitance and the desired image. The first objective function is the mean square error, which is concerned with minimizing the error between the forward solution of the obtained solution and the measured capacitance vector. The other three objective functions are the entropy, smoothness, and 3D to 1D and 2D matching functions. The entropy function is optimized toward an image with maximum information, the smoothness function is optimized for obtaining a solution with minimum image noise, and the 3D to 1-2D matching functions is for assuring the consistency between 1-2D solutions and the required 3D solution. Additional constraints are included as objective functions to assure obtaining the most

possible optimized image. The objective functions are optimized based on a Hopfield neural-network without any prior information.

### Electrostatic Tomography

An extension of the ECVT system is developed through static charge imaging of the charged particulates in the fluidized bed system. The static charged imaging is aimed at providing a 3D map of charges in the system based on the ECVT technology, as well as eliminating the effect of charges on capacitance measurements toward a more accurate ECVT system. In this study, the results are provided based on the ECVT technology alone without regard to the static charge effect.

## EXPERIMENTAL SETUP

A plexiglas fluidized bed of 0.1 m ID and 1.9 m in height is applied in this study, as shown in Fig. 1(a). A porous plate with a pore size of 20 μm and a fractional free area of 60% is employed as a distributor. A two-stage cyclone separates gas and particles and is installed in the freeboard of each fluidized bed. Details of the experimental setup have been reported elsewhere (Du et al., 2003). A differential pressure transducer is installed to measure the pressure drop and the overall voidage of the fluidized bed. The local solids concentration is measured by the optical fiber probe (Du et al., 2003). Both of the Geldart Group A particles (FCC catalyst with a mean diameter of 60 μm and a density of

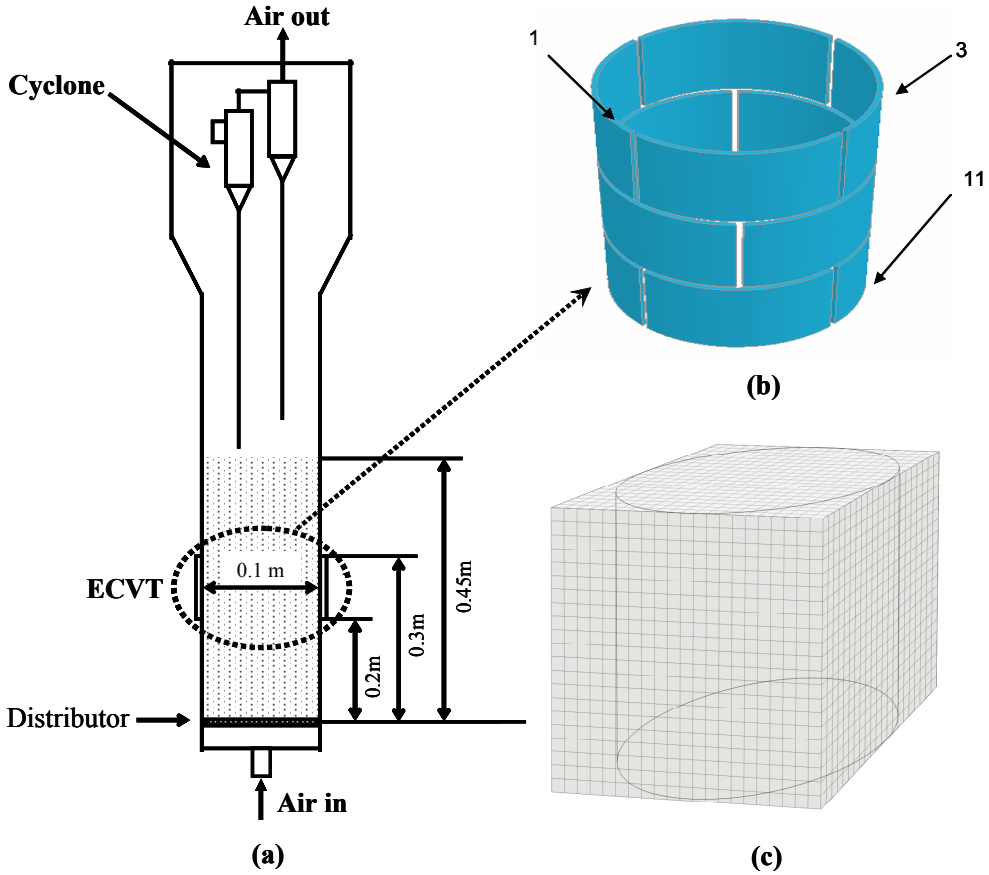


**Fig. 1 Diagram of the 0.1 m ID fluidized bed with the ECVT system: (a) fluidized bed; (b) capacitance esensor design; (c) volume image digitization**

The 12th International Conference on Fluidization - New Horizons in Fluidization Engineering, Art. 57 [2007]

1400 kg/m$^3$) and Group B particles (glass beads with a mean diameter of 200 μm and a density of 2500 kg/m$^3$) are employed in the experiments.

The ECVT system comprises of the capacitance sensor, sensing electronics for data acquisition, and a computer system for image reconstruction. The fundamental concept of the electrical capacitance sensor design for the ECVT is to distribute equally the electrical field intensity (sensitivity) all-over the three-dimensional space (control volume). This concept relates to the sensitivity variance (the difference between the maxima and minima) and the sensitivity strength (the absolute magnitude). A 12-electrode rectangular sensor arranged in triple planes as shown in Fig. 1(b) is applied and its performances for 3D volume imaging are evaluated. The choice of the electrode number is based on the data acquisition system available for experiment, which is, but not limited to, 12 channels. For the rectangular sensor, the electrodes are arranged in one plane shifted to another to distribute the electrical field intensity more uniformly in the axial direction and to increase the radial resolution up to twice the radial resolution of 4-electrode sensor. The radial resolution of the rectangular sensor with this electrode arrangement, thus, equals to 8-electrode sensor per plane. The length of sensing domain is 10 cm. The data acquisition system is capable of capturing image data up to 80 frames per second. There are 66 combinations of independent capacitance measurements between electrode pairs from 12-electrode sensor systems.

The ECVT involves tasks of collecting capacitance data from electrodes placed around the wall outside the vessel (forward problem) and reconstructing image from the measured capacitance data (inverse problem). A multi-criterion optimization based image reconstruction technique developed earlier by the authors (Warsito and Fan, 2001) for solving the inverse problem of 2D ECT is extended to solve the inverse problem of the ECVT. The optimization problem finds the image vector that minimizes simultaneously the four objective functions: negative entropy function, least square errors, smoothness and small peakedness function, and 3-to-2D matching function. It is important to note that in addition to the least square error objective function, all the other functions involved in the reconstruction process collectively define the nature of the desired image based on the analysis of the reconstructed image. Thus, the error, which is generated from the linearized forward solver and propagated to the reconstructed image through the least square objective function, is minimized with the other objective functions applied. Based on the neural network model, the values of the multi-objective functions are minimized simultaneously and the reconstruction problem of the multi-criteria optimization is solved. Details of the image reconstruction technique of the ECVT are described elsewhere (Du et al., 2005; 2006; Warsito et al., 2006). The image is reconstructed on 20x20x20 resolution based on the algorithm described above. The volume image digitization is shown in Fig. 1(c).

## RESULTS AND DISCUSSION

Figure 2 shows the snapshot of the tomography volume image of a gas-solid fluidized bed with 200 μm glass beads at a gas velocity of 0.2 m/s. The 3D solids concentration

distribution in the bed is obtained by the ECVT technique, as shown in Fig. 2 (a).



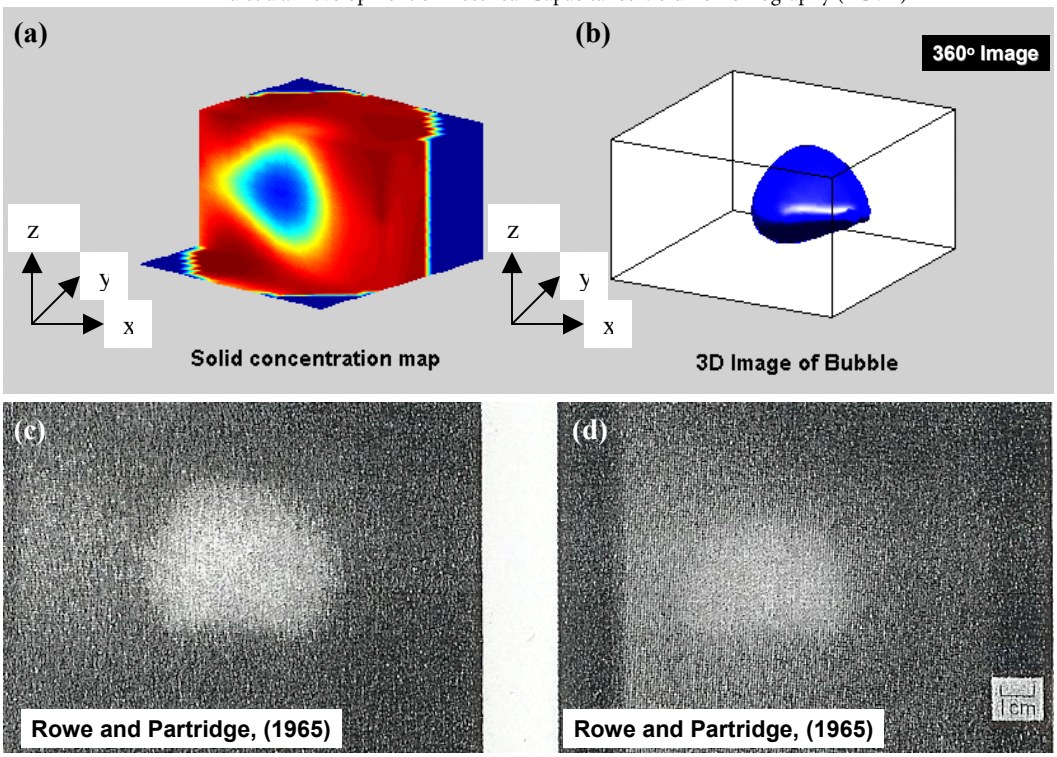


**Fig. 2 Real time 3D qualitative image of a bubble in a gas-solid fluidized bed with Group B particles ($d_p$ = 200 μm; $\rho_p$ = 2500 kg/m$^3$). (a), (b) image from ECVT; (c), (d) image from X-ray photograph**

The color image from blue to red represents the solids concentration spanning from low (empty bed) to high (packed bed). A bubble with spherical cap shape is clearly observed in Fig. 2 (b), which is the 3D iso-surface image obtained by setting the cut-off boundary of 25 % (solids concentration) in the solids concentration distribution profile shown in Fig. 2 (a). The cut-off boundary in Fig. 2 (b) is the same as that used for the quasi-3D image of the bubble in a gas-solid fluidized

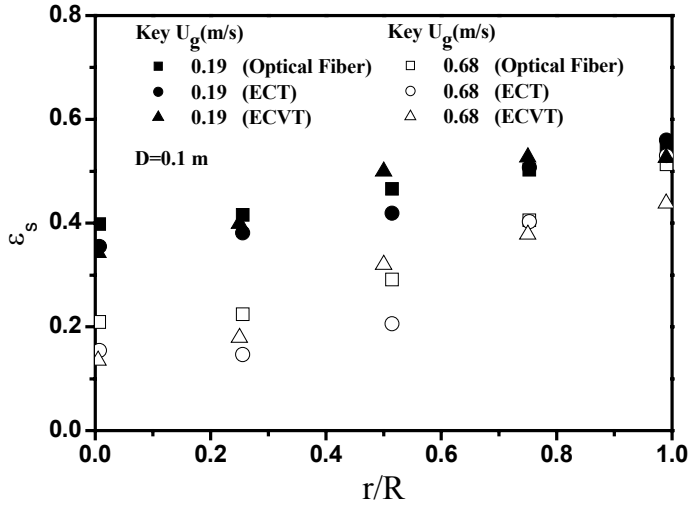


**Fig. 3 Radial profiles of time-averaged solids concentration in a gas-solid fluidized bed with FCC particles ($d_p$ = 60 μm; $\rho_p$ = 1400 kg/m$^3$) obtained by ECVT, ECT and optical fiber probe**

bed obtained by ECT technique (Du et al., 2003). The 3D bubble shape obtained by the ECVT technique is consistent with the quasi-3D bubble obtained by the ECT technique (Du et al., 2003). (bubble size and bubble velocity). Figure 2 (c) and (d) shows the X-ray photography of the bubble in the gas-solid fluidized bed with crushed coal particles ($d_p$ = 530 μm; $\rho_p$ = 1250 kg/m$^3$) and magnesite particles ($d_p$ = 2800 μm; $\rho_p$ = 2930 kg/m$^3$) respectively (Rowe and partridge, 1965). The similarity of the images confirms the accuracy and fastness in real-time volume-imaging of moving dielectric objects in the gas-solid fluidized bed by ECVT technique. Figure 3 shows the comparison of the time-averaged solids concentration profiles at different radial positions measured by ECVT, ECT and the optical fiber probe in a 0.1 m ID fluidized bed for

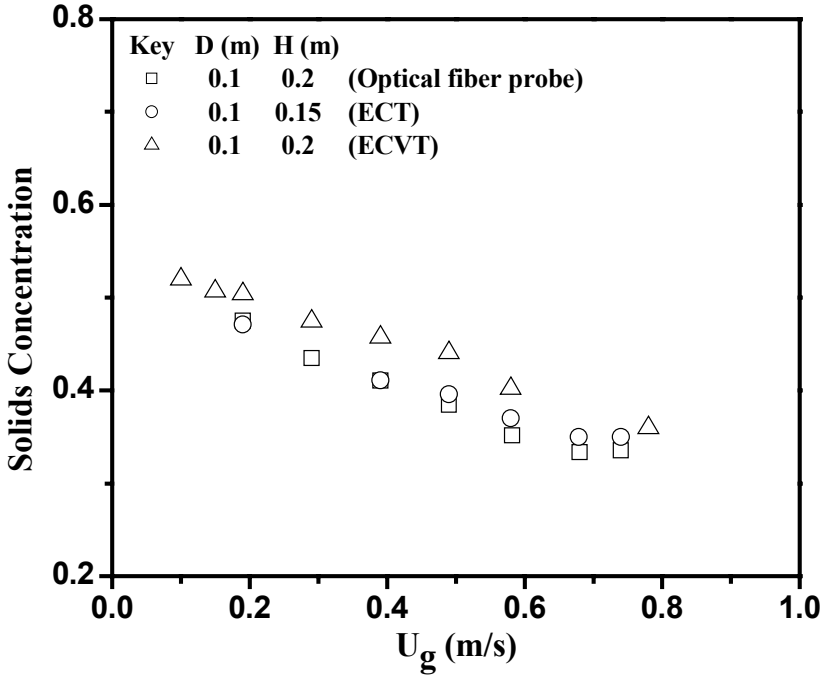


**Fig. 4 Comparison of time-averaged cross-sectional averaged solids concentration in a gas-solid fluidized bed with FCC particles ($d_p$ = 60 μm; $\rho_p$ = 1400 kg/m$^3$) obtained by ECVT, ECT and optical fiber probe**

FCC particles in both the bubbling ($U_g$ = 0.19 m/s) and turbulent regimes ($U_g$ = 0.68 m/s). At the center of the bed, the solids concentration measured by the ECVT is comparable to that measured by the ECT. The solids concentration measured by the optical fiber is larger than that measured by the ECVT and the ECT. The difference between the optical fiber probe and the tomography techniques is larger at higher gas velocities in the turbulent regime. Due to the presence of bubbles at the central region of the bed and the low solids concentration in the bubble phase, the solids concentration measured by the optical fiber probe reflects not only the solids in the bubble phase but also the dense solids surrounding the bubble phase when an optical fiber probe is placed in a bubble. The light-reflection effect of the solid particles in the bed is enhanced

with the increase of the gas velocity, resulting in a higher solids concentration measured by the optical fiber probe at higher gas velocities. At the intermediate region at *r/R* is around 0.5, the solids concentration measured by the ECVT is higher than that measured by the ECT and the optical fiber probe. The solids concentration at this region increases largely along the radius from the central to the wall regions. The relatively low spatial resolution of the ECVT (20×20) compared to that of the ECT (32×32) leads to the higher solids concentration measured by the ECVT. At the wall region, the solids concentrations measured by ECVT, ECT and optical fiber probe are comparable, although solids concentration obtained by the ECVT is slightly smaller due to the low spatial resolution. Though the time averaged solids concentration at different radial positions are somewhat different, the time averaged cross-sectional solids concentrations measured by ECVT, ECT and optical fiber probe are comparable as shown in Fig. 4. The light-reflection effect on the solids concentration at the central region measured by optical fiber probe does not significantly alter the overall solids concentration in a bed cross-section. It is observed that the solids concentrations measured by the ECVT technique are slightly higher than those measured by ECT and optical fiber probe. It can be attributed to the "fuzzy" effect due to the relatively low spatial resolution. Note that the ECT and ECVT provide 2D and 3D images respectively.

ECVT has been introduced in this study as a successful tool for imaging and measuring of solid concentrations in particulate systems. The ECVT technology is being accepted as a favorable measuring tool in many fluidized beds applications due to its safety, feasibility, and ease of operation.

## REFERENCES

Warsito, W., Marashdeh, Q., and Fan, L.-S., (2006), Electrical Capacitance Volume Tomography (ECVT), *IEEE Sensors Journal,* **Submitted**.

Fan, L.-S., Warsito, W., Marashdeh, Q., Park, A.-H. A., and Du, B., (2006), Electrostatic Tomography for Multiphase Process Imaging, Proceedings of 5th World Congress on Particle Technology, Orlando, Florida USA, April 23-27, 2006.

Du, B., Warsito, W., and Fan, L.-S., (2003), Bed non-homogeneity in turbulent gas-solid fluidization, *AIChE J.*, **49** (5), 1109-1126.

Du, B., Warsito, W., and Fan, L.-S., (2005), Transient 3-dimensional behavior of gas-solid fluidization measured using electrical capacitance volume tomography (ECVT), AIChE Annual Meeting, Conference Proceedings, Cincinnati, OH, United States, Oct. 30-Nov. 4.

Rowe, P.N., Patridge, B.A., and Lyall, E., (1964), Cloud formation around bubbles in gas fluidized beds, *Chemical Engineering Science*, **19**, 973-985.

Warsito, W., and Fan, L.-S. (2001), Neural network based on multi-criteria optimization image reconstruction technique for imaging two- and three-phase flow systems using electrical capacitance tomography, *Meas. Sci. Technol.*, **12**, 2198-2210.

Du, B., Warsito, W., and Fan, L.-S., (2006), Imaging the Choking Transition in Gas-Solid Risers Using Electrical Capacitance Tomography, *Industrial & Engineering Chemistry Research*, **45** (15), 5384-5395.